International Journal of Thin Films Science and Technology

http://dx.doi.org/10.18576/ijtfst/110209

Solar Light Induced Photo Catalytic Properties of α-Fe_2O_3 Nanoparticles for Degradation of Methylene Blue Dye

Amanullakhan Pathan[1], *Sandip H. Bhatt*[2], *Shailesh Vajapara*[3,*] *and C. P. Bhasin*[3]

[1]Shri Sarvajanik Science College (PG), Mehsana-384001, India
[2]Chemical Engineering Department, L.D. College of Engineering, Navarangpura, Ahmedabad-380009, India
[3]Department of Chemistry, Hemchandracharya North Gujarat University, Patan- 384265, India

Received: 22 Feb. 2022, Revised: 2 Apr. 2022, Accepted: 12 Apr. 2022
Published online: 1 May 2022

Abstract: The present work describes α-Fe_2O_3 nanoparticles are prepared by chemical displacement method using CTAB as a stabilizing agent. Glutaric acid as fuel and metal salt like ferrous sulphate was used in synthesis. The structural, morphological, metal percentage and optical properties of as synthesized nanoparticles are investigated by using x-ray diffraction (XRD), UV-Visible Spectra; field emission gun Scanning electron microscopy (FEG-SEM) with EDS, Fourier transforms infrared spectroscopy (FTIR), High-resolution Transmission electron microscopy (HR-TEM) and Photoluminescence Spectroscopy (PL). The photocatalytic degradation of Methylene Blue dye was measured by visible absorption spectroscopy. To obtain the most favorable conditions for degradation of MB dye, the effect of various experimental parameters, i.e., pH, amount of nanoparticles, concentration of dye and light intensity on the rate of reaction was studied. A tentative mechanism for the photocatalytic degradation of Methylene Blue was proposed. Photocatalytic degradation of Methylene Blue dye followed pseudo first-order kinetics. It was found that the dye degradation gave the best results at a pH of 6.0, and using a 70 mW•cm^{-2} light intensity with 0.3 g of α-Fe_2O_3 nanoparticles. At room temperature, the photocatalytic degradation of Methylene Blue dye was observed about 92.3%.

Keywords: Nanoparticles, α-Fe_2O_3, XRD, FTIR, UV-Vis, FEG-SEM, EDAX, HR-TEM.

1 Introduction

Iron oxides are very useful materials with three common forms likes hematite, maghemite, and magnetite [1]. Among them, hematite (α-Fe_2O_3) is most stable under ambient conditions and the most environmentally friendly n-type functional material and semiconductor [2,3,4,5] (e.g., 2.1*eV*). Therefore, it has wide applications in many fields such as catalysts, electrodes, gas sensors, pigments, magnetic materials, clinical therapy and diagnosis [6,7,8,9] etc. They are also used as dye sensitized solar cells [10], lithium-ion batteries [11], gas sensors [12,13], red pigments [14], anticorrosive agents [15], high density magnetic recording media [16], catalysts [17], magnetic resonance imaging (MRI) contrast agents [18], dye degradation [19,20], printing ink [21] and nanofillers [22]. As a result, many methods including sol–gel method [23], hydro thermal synthesis [24], micro-emulsion technique [25], solvothermal synthesis [26], high energy ball milling [27], thermal decomposition method [9], in situ synthesis [28], vapor–solid growth technique [29], modified Pechini method [30], solution combustion method [31], method [32], Precipitation method [33], template synthesis [34], and sonoelectro chemical anodization method [35] have been developed to synthesize α-Fe_2O_3 nanomaterials with different morphologies and nanostructures. Review of literature reveals that the size and morphology of α -Fe_2O_3 nanoparticles strongly depend on the composition of precursors, pH of the solution and rate of heating/cooling during synthesis. Thus, a significant attention must be paid on the optimization of experimental parameters to avoid the formation of undesired products [36, 37, and 38]. 8 years ago, Peng [3] *et al*. have reported hydrothermal process of α-Fe_2O_3 nanoparticles by using ferric hydroxide suspension and excess amount of NaOH. A synthesized nanoparticle was homogeneously sized and hexagonal in shape. Wang [39] *et al*. have reported Iron oxide (α-Fe_2O_3) nanoparticles were synthesized by a simple hydrothermal synthesis

*Corresponding author E-mail: shaileshvajapara91@gmail.com

method using only Fe $(NO_3)_3.9H_2O$ and NH_4OH as raw materials.

The present work describes the synthesis of α-Fe_2O_3 nanoparticles by using Chemical Displacement Method. The present method is very low cost and very easy to prepare α-Fe_2O_3 nanoparticles. In this method, we have used Cetyl trimethyl ammonium bromide (CTAB) as a stabilizing agent, Glutaric acid as fuel and ferrous sulphate as a metal salt. Synthesized α-Fe_2O_3 nanoparticles are characterized by various analytical techniques like X-ray diffraction (XRD), UV-Visible Spectra; field emission gun Scanning electron microscopy (FEG-SEM) with EDS, Fourier transforms infrared spectroscopy (FTIR), High-resolution Transmission electron microscopy (HR-TEM) and Photoluminescence Spectroscopy (PL). The Photocatalytic activity of synthesized α-Fe_2O_3 nanoparticles was investigated by photo degradation of Methylene Blue as a pollutant from industrial effluent.

2 Experimental

2.1 Materials

AR-grade ferrous sulphate, Glutaric acid, Cetyl trimethyl ammonium bromide (CTAB), methanol and Methylene Blue dye (MB) were used as received from the s.d fine chemicals (India). All reaction was performed using double Distilled water.

2.2 Synthesis of Fe_2O_3 nanoparticles

In the following chemical displacement method, α-Fe_2O_3 nanoparticles were prepared by reaction of 1 mol of $FeSO_4$ and 2 mol of Glutaric acid. Ferrous sulphate was dissolved in 30 ml double distilled water and was a transfer to a round bottom flask. In another beaker 2 mol of Glutaric acid and 1 mol of Cetyl trimethyl ammonium bromide (CTAB) were dissolved in 50 ml of methanol. This whole mixture was added drop wise in ferrous sulphate solution and the resulting mixture was refluxed at around 65 ^{0}C for 4 hrs. After 4 hrs, colour of the solution changed from light green to yellow. Yellow solution was cooled at room temperature. The nanoparticles were centrifuged. The nanoparticles were washed with double distilled water for 5 times to remove the impurities. For Calcination, these nanoparticles were transferred to silica crucible and kept in muffle furnace at 600 ^{0}C for 3 hrs. After this process the Brown colour crystalline nanoparticles of α-Fe_2O_3 were obtained.

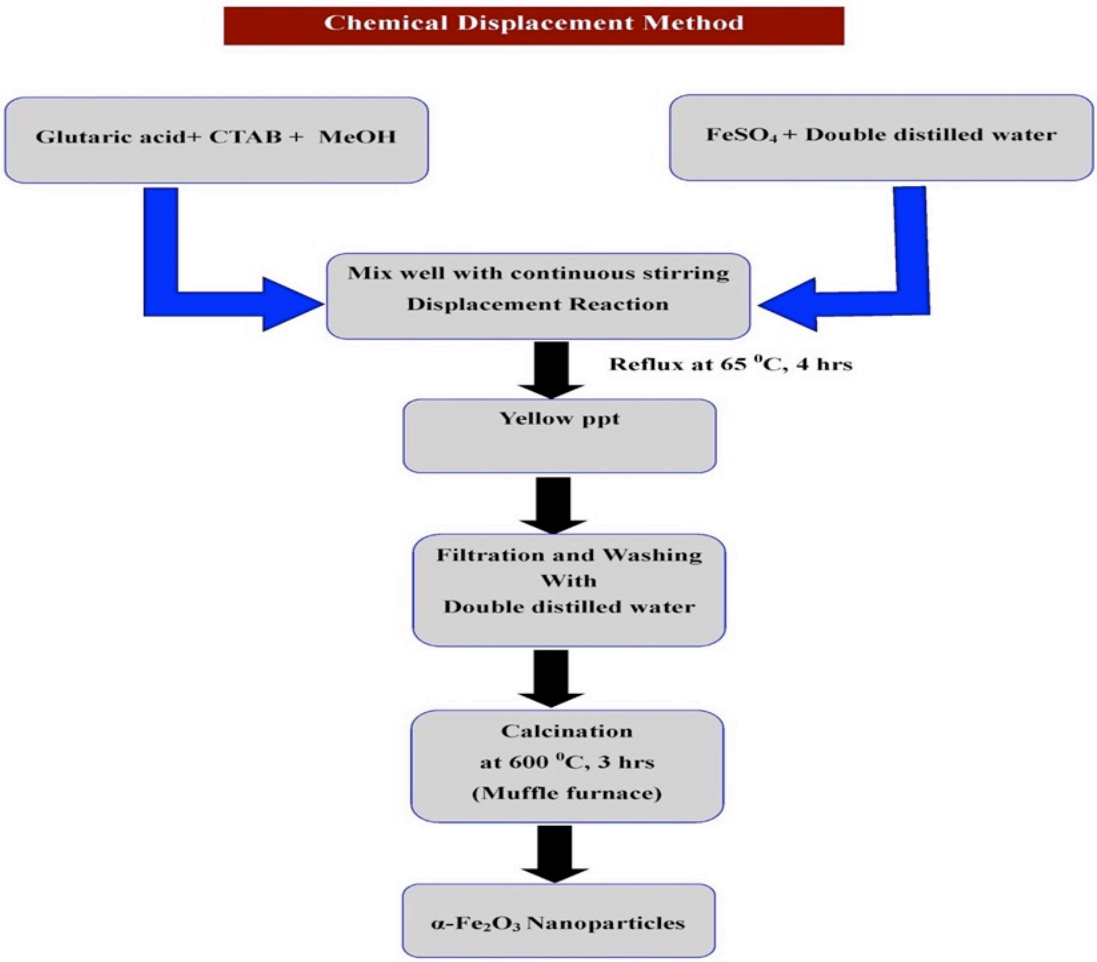

Fig.1: Schematic diagram for the synthesis of α-Fe_2O_3 Nanoparticles.

2.3 Instruments used for Characterization of synthesized α-Fe_2O_3 particles

The synthesized α-Fe_2O_3 samples were characterized by using different analytical techniques likes UV-Vis spectra, Fourier transform infrared (FTIR) spectra, X-ray powder diffraction (XRD) analysis, Field emission gun scanning electron microscopy (FEG-SEM) with EDS, High-resolution Transmission electron microscopy (HR-TEM), Photoluminescence spectra. The Photocatalytic Properties of α-Fe_2O_3 nanoparticles were recorded by using UV–1800, Shimadzu spectrophotometer.

2.4 Photocatalytic activities

The photocatalytic activity of the nanocomposites was assessed by monitoring decolorization of Methylene Blue (MB) in the presence of visible light. Methylene Blue (MB) is Phenothiazine dye that extensively used in dyeing, printing industries. It has severe toxic effects on the human health. Although there are many studies on adsorption/photo degradation of Methylene Blue using different reductants, it is of interest to investigate the environmentally kindly α-Fe_2O_3 nanoparticles. α-Fe_2O_3 was interacted with Methylene Blue (MB) solution at different pH (3-6.5), different amount of NPs, different concentration of dye and light intensity.

3 Results and Discussion

3.1 Characterization of α-Fe_2O_3 nanoparticles

3.1.1 UV-Vis spectrum of α-Fe_2O_3 nanoparticles:

The Figure-2 shows that UV–Vis absorption spectrum of synthesized α-Fe_2O_3 nanoparticles dispersed in the distilled water using by Probe sonication method. The UV absorption peak was observed nearby 350 nm also the previous report shown the absorption peak around 350-400 nm. It confirms that formation of α-Fe_2O_3 Nanoparticles, while their found good particle size distribution and consistency of particles is confirmed based on the good width of this absorption peak [40].

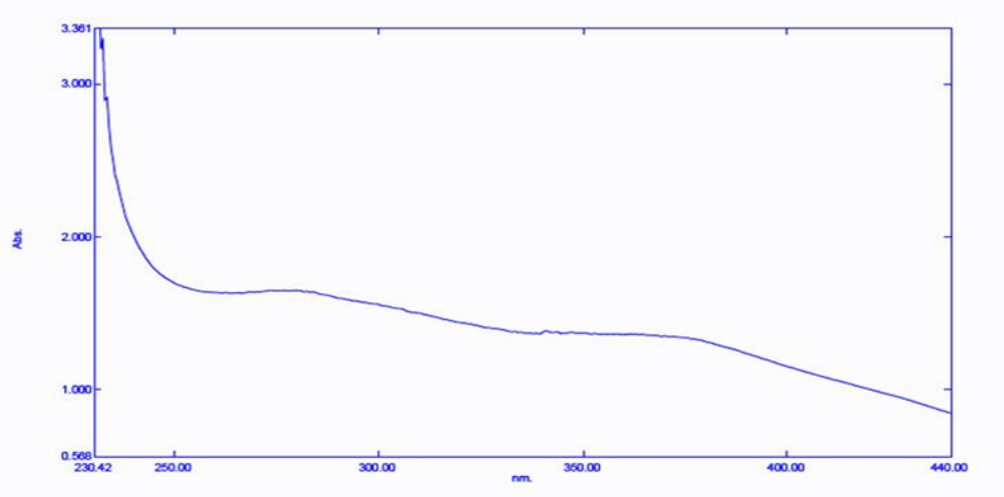

Fig. 2: UV-Vis spectrum of synthesized α-Fe_2O_3 nanoparticles.

3.1.2 FTIR spectra of α-Fe_2O_3 nanoparticles:

FT-IR is an important characterization technique to identify the functional groups present in a material. **Figure-3** Shows the FT-IR transmittance spectrum of α-Fe2O3 nanoparticles recorded in the frequency range 400-4000 cm^{-1} using Bruker (ALPHA-T) FTIR spectrometer at room temperature. The characteristic absorption bands (Fe-O bonds) occur at 472 cm^{-1} and 831 cm^{-1}. The broad peak around 3363 cm^{-1} is due to O-H stretching vibration and 1193 cm^{-1} corresponds to O-H deformation band. The peak at 2339 cm^{-1} is attributed to the presence of adsorbed water molecule (H-O-H) in the sample [41,42].

3.1.3 XRD spectra of α-Fe_2O_3 nanoparticles:

The synthesized α-Fe_2O_3 nanoparticles by using chemical displacement process were characterized by X-ray powder diffraction (XRD) to evaluate and study their structure. XRD spectra of the synthesized α-Fe_2O_3 nanoparticles are shown in **Figure-4**. As seen, the prepared nanoparticles have a good crystallinity and all diffraction peaks are in

good agreement with hexagonal structures and peaks indexed in this pattern is consistent with the α-Fe_2O_3 pattern (JCPDS Card No. 33-0664) [43,44,45].

The average particle size of the α-Fe_2O_3 Nanoparticles was estimated by the Scherrer equation.

$$\mathbf{D} = \frac{0.9\lambda}{\beta\, Cos\theta}$$

Where, D is the average crystallite size of the α-Fe_2O_3 nanoparticles, θ is the peak position angle, λ is is

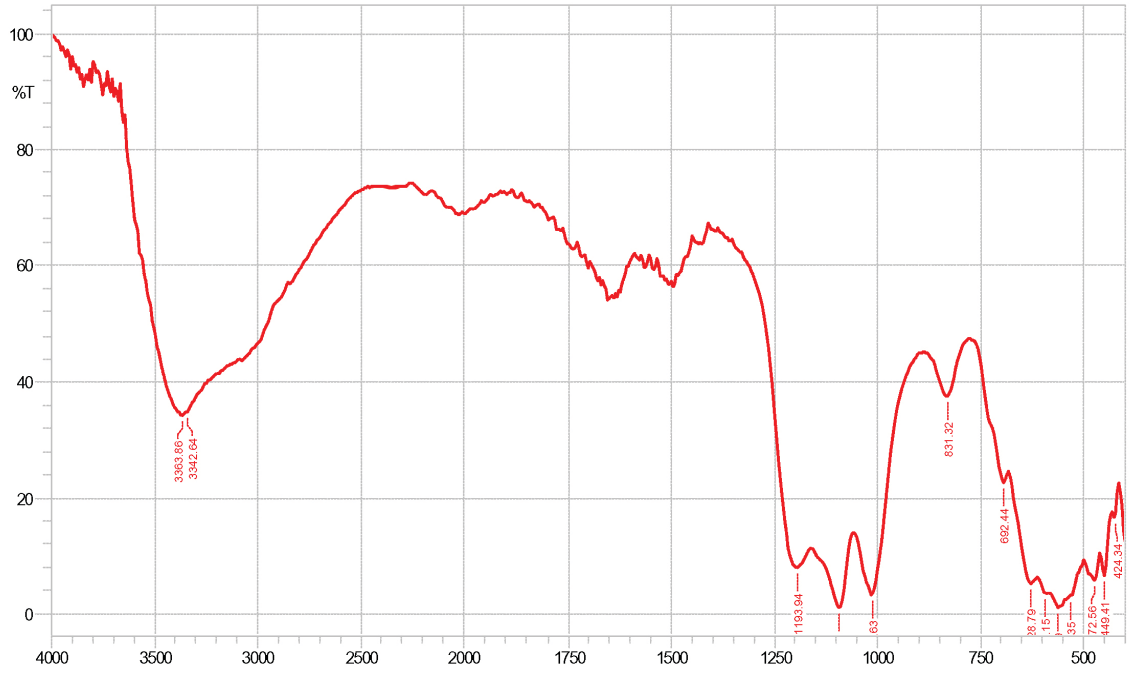

Fig.3: FTIR spectrum of α-Fe_2O_3 nanoparticles.

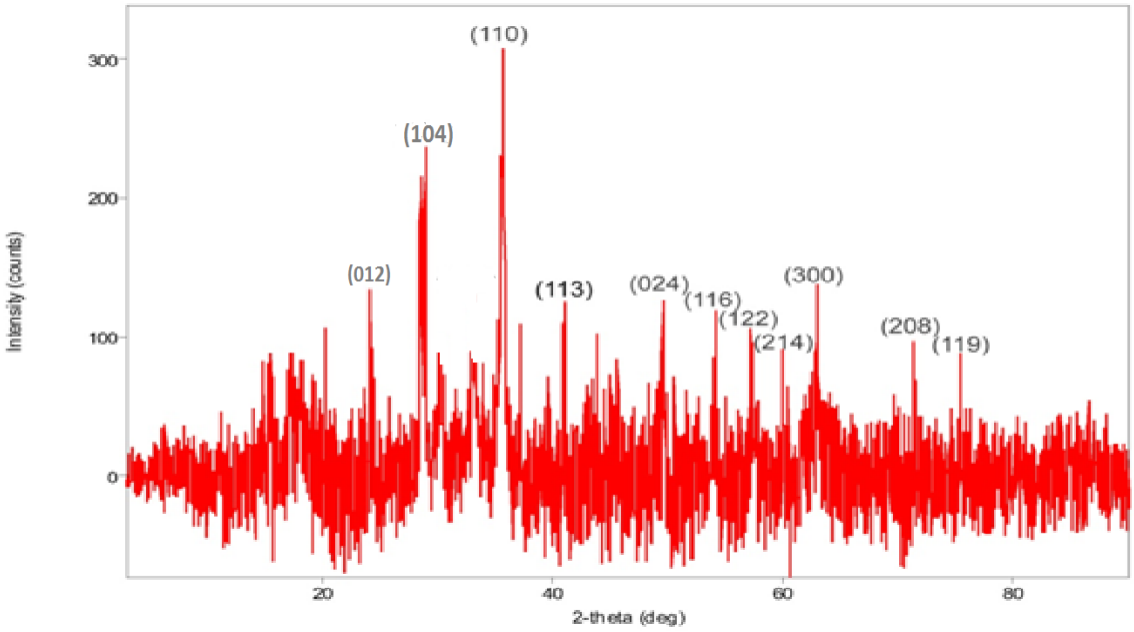

Fig.4: X-ray diffraction spectra of α-Fe_2O_3 nanoparticles.

Wavelength of the X-ray radiation and β is the full width at half-maximum (FWHM) of the XRD corresponding Peaks. The results show that the average crystalline size of the obtained α-Fe_2O_3 nanoparticles was 21.1 nm.

3.1.4 Field emission gun scanning electron microscope (FEG-SEM) with EDS of α-Fe_2O_3 nanoparticles:

Field Emission Gun Scanning Electron Microscopy (FEG-SEM) analysis was performed by JEOL JSM-7600F model and showed morphological features and examine the surface morphology and distribution of nanoparticles. The **Figure-5** shows FEG-SEM micrographs of the α-Fe_2O_3 nanoparticles existing the homogenous distribution of nano particles. However, it should be noted that uniform in size and shape. FEG-SEM images (**Figure-5**) represented the hexagonal shape of α-Fe_2O_3 nanoparticles. The Stoichiometric composition of α-Fe_2O_3 nanoparticles is shown in the EDS profile.

Figure-5 depicts FEG-SEM images of α-Fe_2O_3 nanoparticles. From the SEM analysis, it was observed that the nanoparticles are uniform in particle size and the α-Fe_2O_3 nanoparticles morphology was observed like hexagonal in shape.

The EDS spectra obtained for α-Fe_2O_3 nanoparticles (**Figure-6**). EDS spectra of α-Fe_2O_3 show the peaks for Iron and Oxygen elements indicating the good development of α-Fe_2O_3 nanoparticles. Peak indexing of the elements is Oxygen 0.5 keV and Iron 0.8, 2.2, 6.4, 7.2 keV. The compositions in the mass percentage of the elements are Oxygen 30.53 % and Iron 62.96 %. The above data indicate no impurities in synthesized α-Fe_2O_3 nanoparticles.

3.1.5 High resolution Transmission electron microscope (HR-TEM) of α-Fe_2O_3 nanoparticles:

High resolution Transmission Electron Microscopy (HR-TEM) was performed using Tecnai G2-F30 model. Crystalline Size and shape morphology studied by HR-TEM.

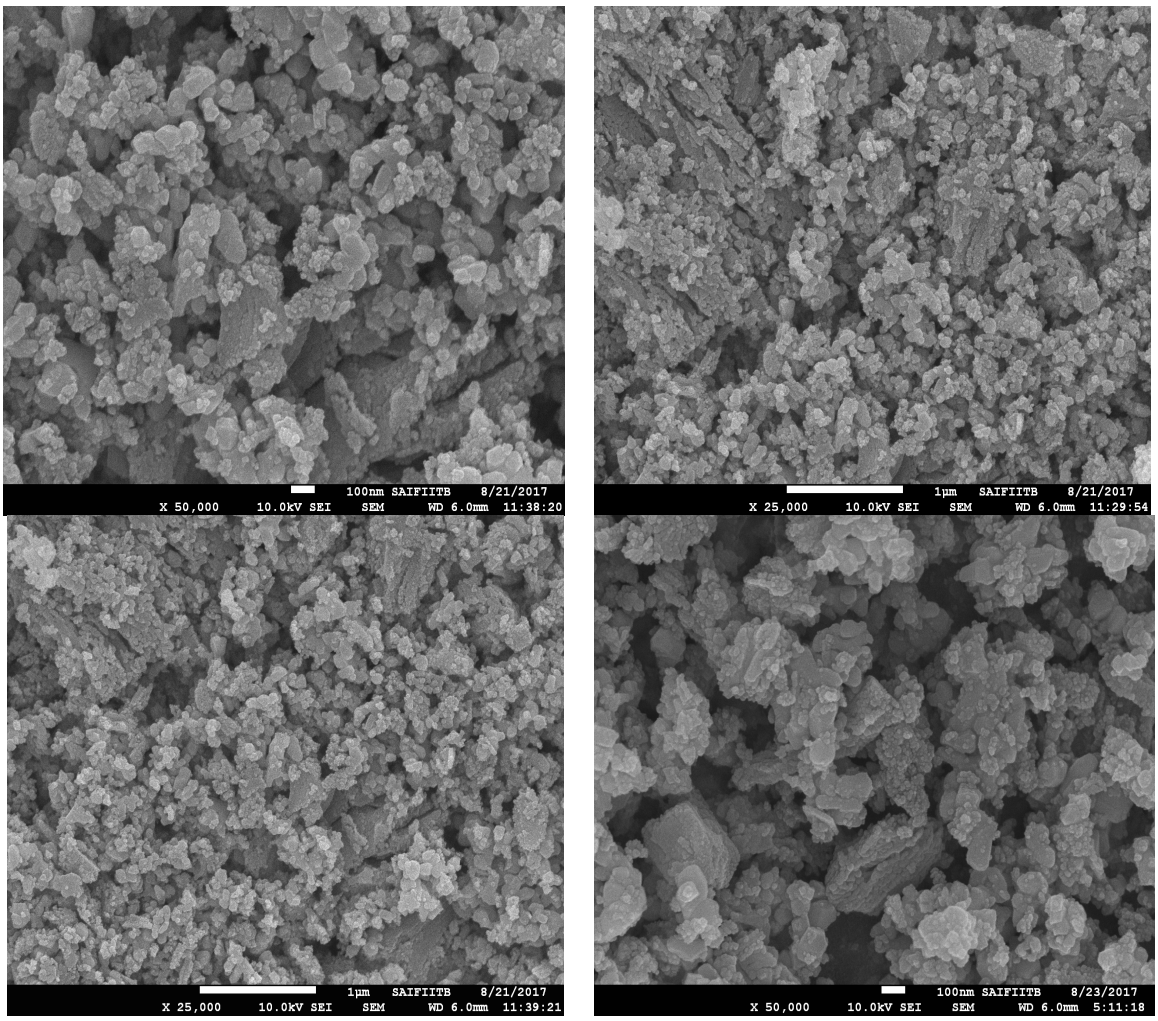

Fig.5: FEG-SEM spectra for α-Fe_2O_3 nanoparticles.

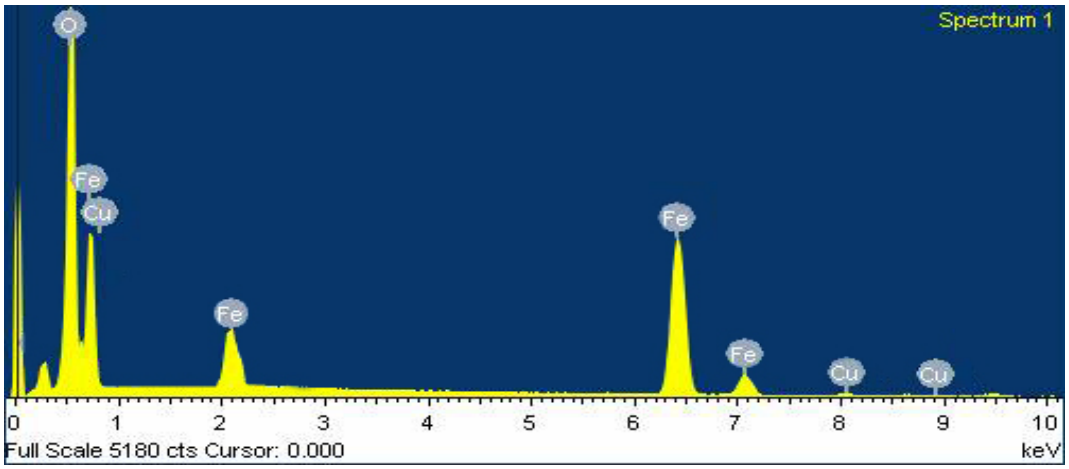

Fig.6: EDAX spectra for α-Fe_2O_3 nanoparticles.

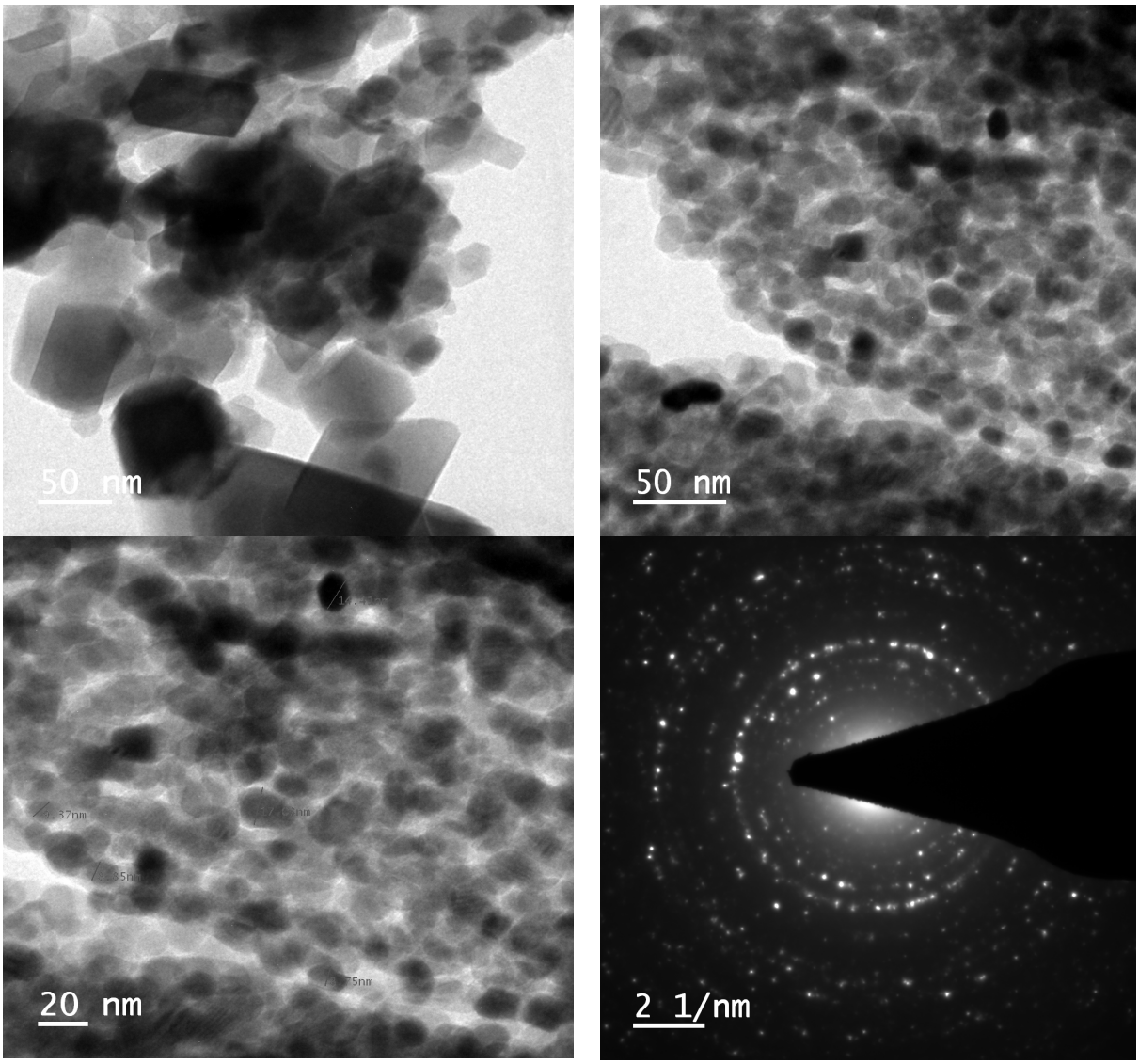

Fig.7: HR-TEM images for α-Fe_2O_3 nanoparticles.

Figure-7 highlights the transmission electron microscope (HR-TEM) images of the synthesized samples. The HR-TEM images also show that the particle size of the pure hematite (α-Fe_2O_3) is 21 nm. These HR-TEM observations confirm the small size of the hematite nanoparticles and the obtained values are in good agreement with the size of crystallites calculated from the Scherrer equation. Using the selected area electron diffraction (SAED) pattern with bright circular spots, the crystallinity of the α-Fe_2O_3 nanoparticles was evidenced.

3.1.6 Photoluminescence Spectrum of α-Fe_2O_3 Nanoparticles

The photoluminescence spectrum of α-Fe_2O_3 nanoparticles is shown in the **figure-8**. The excitation wavelength is 340 nm. The emission spectrum shows broad peak around 427 nm. The peaks were attributed to emissions from defect levels. As observed from figure, a sharp emission peak is observed at 427 nm when the samples were excited at 340 nm. The peak position remains constant in all the cases, although a variation in intensity has been recorded. L.E. Mathevula *et al.* have reported an emission at 422 nm in the PL spectra of α-Fe_2O_3 on excitation at 336 nm [46].

3.2 Photocatalytic activities:

α-Fe_2O_3 is a semiconductor with a band-gap of 2.0–2.6 eV and can absorb from visible to UV region of the solar spectrum with assured wavelengths [47,48]. Therefore, α-Fe_2O_3 nanoparticles can be a fine photocatalysis to speedy degradation of dyes. In this case, we evaluated the photocatalytic activities of as-prepared α-Fe_2O_3 nanoparticles under visible light irradiation using Methylene Blue (MB) aqueous solution as model contaminants. The concentration of MB dye in the form of absorbance before and after photocatalytic degradation was measured at 664 nm (λ_{max} value obtained for Methylene Blue dye). A 200 W tungsten lamp (Philips) was used as the visible light source. A cutoff filter was placed between the light and the sample (filled with water) to remove the thermal radiation just to ensure illumination by visible light. The progress of the photocatalytic reaction was observed by taking absorbance at regular time intervals.

The photocatalytic activity of α-Fe_2O_3 nanoparticles was investigated for the degradation of Methylene blue as pollutant from industrial effluents. In the present investigation the Methylene blue solution prepared in double distilled water was used for photocatalytic activity. The values have been depicted in **figure-13**. It was observed that the absorbance of MB dye decreased in presence of photo catalyst and light. The plot has been depicted in **Figure-13**. The plot of absorbance versus time was linear. Hence, the reaction followed pseudo first order kinetics. The pseudo first order kinetic model has been depicted by the following equation:

$$ln\left(\frac{C_0}{C_t}\right) = kt \quad \ldots\ldots\ldots\ldots\ldots (2)$$

Where C_0 and C_t are the concentrations of dye in solution at times 0 and t respectively, and k is the first-order rate constant (min^{-1}). The plot of C/C_0 (the ratio of MB concentration to the initial concentration) versus time is shown in **Figure-13**. As the results reflected after 120 minutes maximum degradation (about 92.3 %) of MB was achieved. This result suggests that α-Fe_2O_3 nanoparticles could be utilized as a good and effective photo catalyst for removal of methylene blue as a pollutant from industrial effluent.

3.2.1 Effect of the amount of α-Fe_2O_3 nanoparticles

The effects of the amount of α-Fe_2O_3 nanoparticles are also likely to affect the process of Methylene Blue dye degradation and therefore, different amounts of nanoparticles were used.

It has been observed that as the amount of nanoparticles was increased, the rate of photo degradation of Methylene Blue also increased as well as the number of active sites. But eventually the rate became almost constant after adding a certain amount (0.3 g) of nanoparticles. This may be due to the fact that, after a certain limit, the increase in amount of α-Fe_2O_3 nanoparticles did not increase the exposed surface area (active sites) of the nanoparticles. It only increased the thickness of the layer, as the bottom of the reaction vessel was covered by the nanoparticles. It may be considered that a kind of saturation point was reached, and that, after this saturation point no effect of amount of nanoparticles was observed.

3.2.2 Effect of pH

The effect of pH on photocatalytic degradation was investigated in the range 3-6.5. It is evident from the Table-10 that the degradation rate of Methylene Blue increases with increasing pH of solution up to 6.0 and above this value of pH, the rate of photocatalytic degradation of Methylene Blue starts decreasing. It may be explained on the basis that at low pH, the Phenothiazine dye was attracted by positively charged surface of nanoparticles, but after a certain limit, further increase in pH turned surface of nanoparticles as negatively charged. Due to presence of lone pairs on two oxygen atoms, Methylene Blue seems to face a force of repulsion from negatively charged surface of the nanoparticles, which results into a decreasing rate of reaction.

3.2.3 Effect of concentration of Methylene Blue

The concentration of dye was varied from 25 ppm to 200 ppm. From the above data, it has been observed that the rate of photocatalytic degradation of MB dye increases with increase in the dye concentration up to 150 ppm. This may

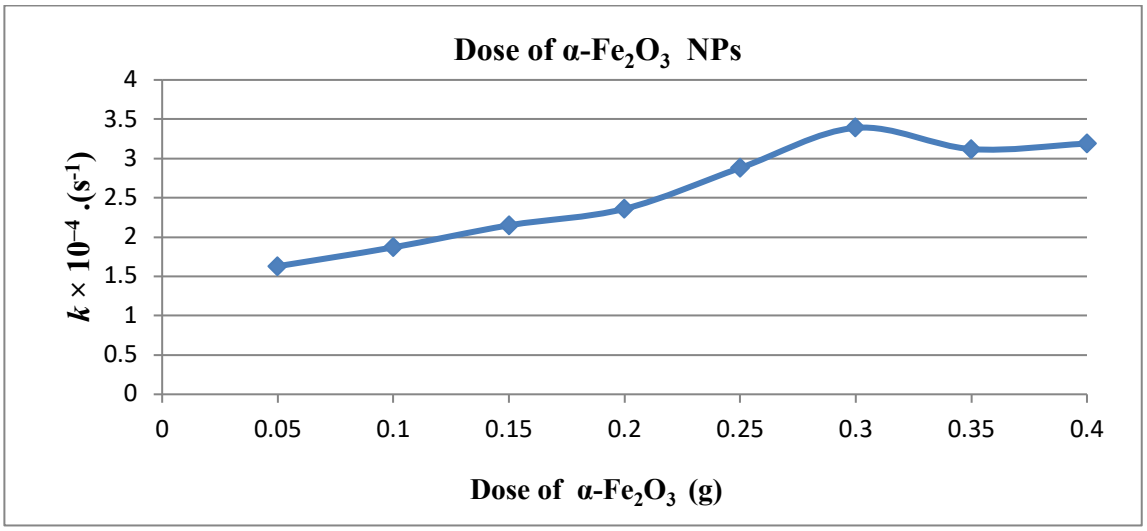

Fig.9: Effective dose of α-Fe_2O_3 nanoparticles.

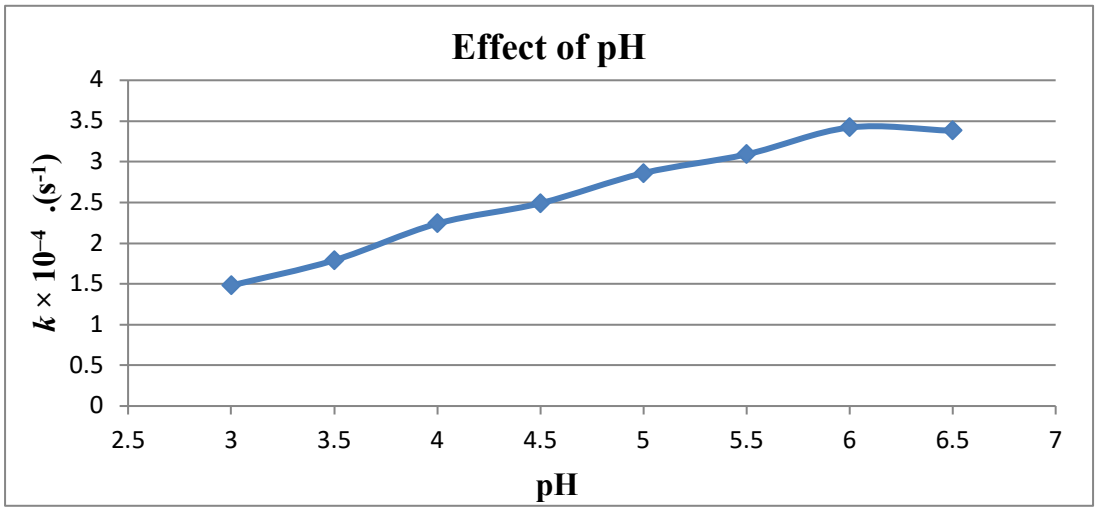

Fig.10: Effect of pH.

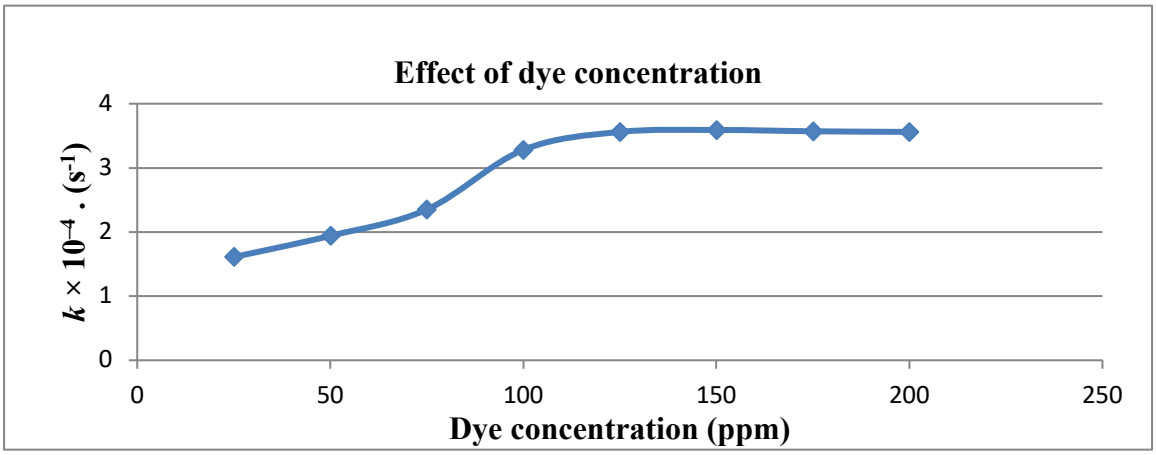

Fig.11: Effect of Dye concentration.

Blue was increased, more dye molecules were available for excitation and following degradation. Hence, an increase in the rate was observed. The rate of photocatalytic degradation was shown to decrease with further increase in the concentration of MB dye. This may be certified to the fact that the dye started acting as a filter for the incident light and it does not permit the desired light intensity to reach the photocatalyst surface in a limited time sphere; thus, decreasing the rate of photocatalytic degradation of Methylene Blue.

3.2.4 Effect of Light Intensity

The effect of the variation of the light intensity on the rate was also investigated and the observations are represented in figure. The experimental data indicate that the degradation action was accelerated as the intensity of light was increased, because any increase in the light intensity increases the number of photons striking per unit time per unit area of the nanoparticles. An almost linear behavior between light intensity and the rate of reaction has been

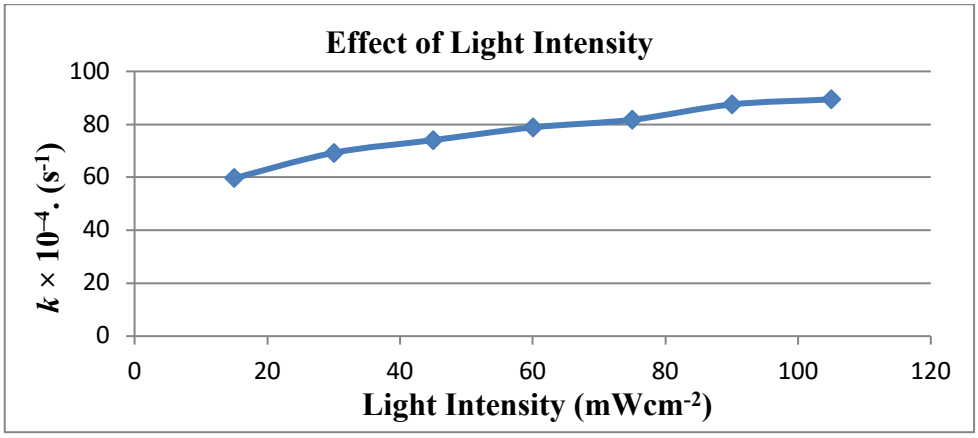

Fig.12: Effect of Light intensity.

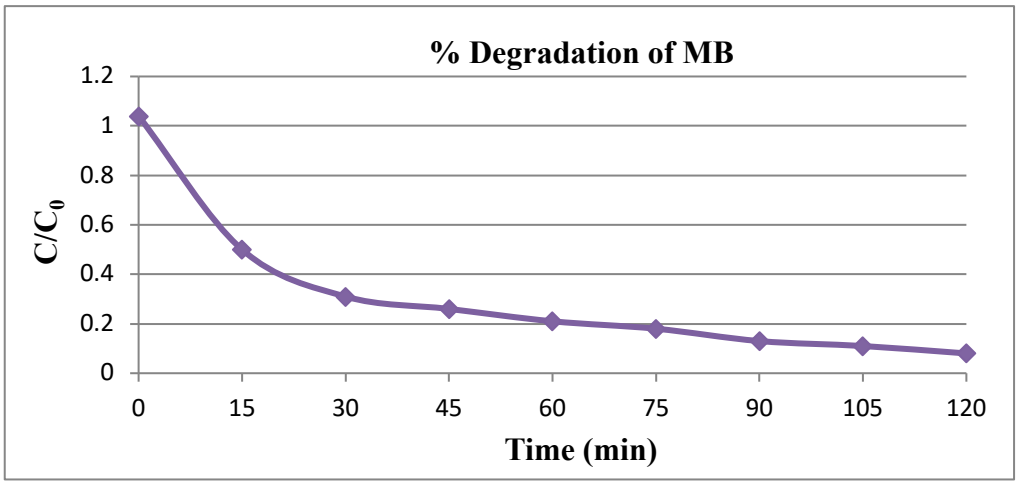

Methylene Blue dye = 150 ppm; α-Fe_2O_3 NPs = 0.3 g,

Light intensity = 70 $mWcm^{-2}$; pH = 6, R.T.

Fig.13: Photocatalytic performance of α-Fe_2O_3 nanoparticles.

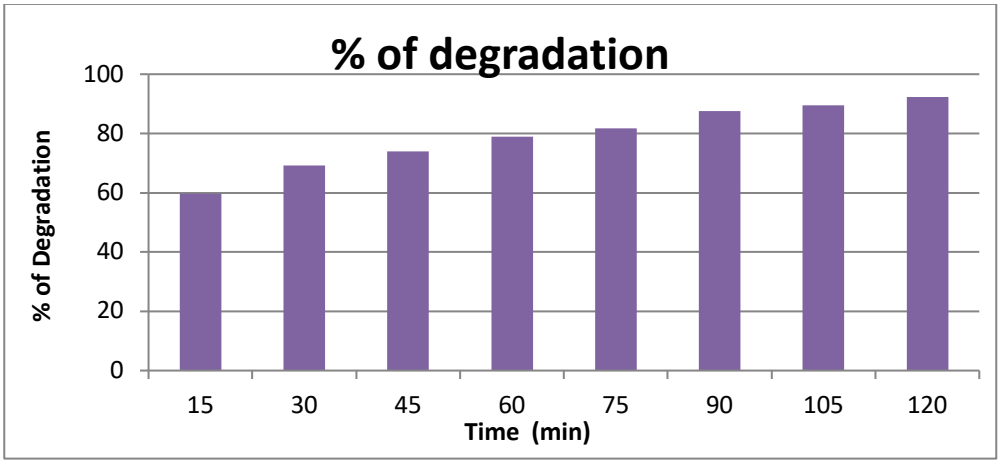

Fig.14: Photocatalytic degradation of Methylene Blue dye.

Observed. However, higher intensities were avoided due to its thermal effects.

3.2.5 Tentative Mechanism of Methylene Blue Photo Degradation

Based on these observations, a tentative mechanism for the photocatalytic degradation of Methylene Blue (MB) is proposed:

$$^1MB_0 \xrightarrow{h\nu} {}^1MB_1 \quad (1)$$

$$^1MB_1 \xrightarrow{ISC} {}^3MB_1 \quad (2)$$

$$SC \xrightarrow{h\nu} h^+(VB) + e^-(CB) \quad (3)$$

$$h^+ + OH^- \longrightarrow {}^{\bullet}OH \quad (4)$$

$$^3MB_1 + {}^{\bullet}OH \longrightarrow {}^3MB_1^-(\text{Leuco form}) \quad (5)$$

$$^3MB_1^-(\text{Leuco form}) \longrightarrow \text{Products} \quad (6)$$

A molecule of Methylene Blue absorbs radiations of a suitable wavelength giving gives rise to its excited singlet state, which then undergoes intersystem crossing (ISC) to give the triplet state of the dye. On the other hand, the semiconducting α-Fe_2O_3 (SC) also utilizes the radiant energy to excite its electron from the valence band to the conduction band; thus, leaving behind a hole. This hole abstracts an electron from OH^- to generate OH radicals. These radicals oxidize the dye to its Leuco form, which may ultimately degrade to harmless products.

4 Conclusions

Hematite α-Fe_2O_3 nanoparticles were successfully prepared by using simple Low-cost Chemical Displacement reaction at most favorable conditions with using CTAB as a stabilizing agent. Synthesized α-Fe_2O_3 nanoparticles by the chemical displacement method were composed of the hexagonal in shape. The composition and structure of the synthesized α-Fe_2O_3 nanoparticles at optimum conditions were characterized by various analytical techniques likes UV-Vis, FTIR, XRD, FEG-SEM with EDS, HR-TEM and Photoluminescence Spectroscopy techniques. The results of present work confirmed the formation of α-Fe_2O_3 nanoparticles. From UV-Vis spectra, absorption peak observed around 350 nm confirms the formation of α-Fe_2O_3 NPs and XRD patterns show that average particles size found 21.1 nm. Photocatalytic Performance of the synthesized α-Fe_2O_3 nanoparticles was studied and the results exposed the potential of the synthesized α-Fe_2O_3 nanoparticles as a photo catalyst in Methylene Blue (MB) dye degradation. Photocatalytic degradation of Methylene Blue was performed in the presence of α-Fe_2O_3 nanoparticles. The degradation rate increased with increasing pH because more hydroxyl ions were present (generating more hydroxyl radicals). It attains maximum rate at pH 6; a further increase in pH above 6 results in a decrease in the rate of the reaction, because of decreasing attraction between the neutral form of the dye and the negatively charged semiconductor surface. Increasing the concentration of Methylene Blue also increased the rate up to a certain value due to the increase in the number of dye molecules, but it shows a declining behavior on further increase of the concentration of dye. This decrease may be attributed to the fact that at higher concentration, the dye may acts as an internal filter for the incident radiations, which decreases the intensity of the incident radiation on the nanoparticles. The results indicate that initially the rate increases with increasing amount of semiconductor but after 0.3 g, the rate becomes virtually constant (saturation

behavior). This may be due to the complete coverage of the bottom of the reaction vessel by the nanoparticles. Any further increase will not add to an increase in the exposed surface area but only increases the thickness of the layer. An increase in the light intensity will increase the number of photons striking α-Fe_2O_3 nanoparticles per unit area per second and as a consequence, the reaction rate increases almost linearly with the increase in light intensity. Scavengers trap the active species by reducing their activity in the solution and as a result reaction rate becomes quite low or reaction almost stops. Here, the participation of •OH as an active oxidizing species was confirmed by using 2-propanol, which is a specific scavenger of •OH. It was observed that the rate of dye degradation was reduced drastically. The optimum reaction conditions were obtained as: pH = 6; [Methylene Blue] = 150 ppm; α-Fe_2O_3 NPs = 0.3 g; contact time = 120 min; light intensity = 70.0 $mWcm^{-2}$. The results showed after optimum reaction conditions maximum degradation (about 92.3 %) of MB was achieved.

References

[1] Fan, H. M., G. J. You, Y. Li, Z. Zheng, H. R. Tan, Z. X. Shen, S. H. Tang, and Y. P. Feng. "Shape-controlled synthesis of single-crystalline Fe2O3 hollow nanocrystals and their tunable optical properties." The Journal of Physical Chemistry C., **113(22)**, 9928-9935, (2009).

[2] Song, Limin, Shujuan Zhang, Bin Chen, Jingjie Ge, and Xicheng Jia. "A hydrothermal method for preparation of α-Fe2O3 nanotubes and their catalytic performance for thermal decomposition of ammonium perchlorate." Colloids and Surfaces A: Physicochemical and Engineering Aspects., **360(1)**, 1-5, (2010).

[3] Peng, Dengfeng, Sadeh Beysen, Qiang Li, Yanfei Sun, and Linyu Yang. "Hydrothermal synthesis of monodisperse α-Fe2O3 hexagonal platelets." Particuology., **8(4)**, 386-389, (2010).

[4] Hua, Jiao, and Jiao Gengsheng. "Hydrothermal synthesis and characterization of monodisperse α-Fe2O3 nanoparticles." Materials Letters., **63(30)**, 2725-2727, (2009).

[5] Sun, Youyi, Guizheng Guo, Binhua Yang, Wei Cai, Ye Tian, Minghong He, and Yaqing Liu. "One-step solution synthesis of Fe2O3 nanoparticles at low temperature." Physica B: Condensed Matter., **406(4)**, 1013-1016, (2011).

[6] Wu, Yuanting, and Xiufeng Wang. "Preparation and characterization of single-phase α-Fe2O3 nano-powders by Pechini sol–gel method." Materials Letters., **65(13)**, 2062-2065, (2011).

[7] Zhan, Sihui, Dairong Chen, Xiuling Jiao, and Shusheng Liu. "Facile fabrication of long α-Fe2O3, α-Fe and γ-Fe2O3 hollow fibers using sol–gel combined co-electrospinning technology." Journal of colloid and interface science., **308(1)**, 265-270, (2007).

[8] Sun, Lingna, Minhua Cao, and Changwen Hu. "Synthesis and magnetic properties of hollow α-Fe2O3 nanospheres templated by carbon nanospheres." Solid State Sciences., **12(12)**, 2020-2023, (2010).

[9] Darezereshki, Esmaeel, Fereshteh Bakhtiari, Mostafa Alizadeh, and Mohammad Ranjbar. "Direct thermal decomposition synthesis and characterization of hematite (α-Fe2O3) nanoparticles." Materials Science in Semiconductor Processing., **15(1)**, 91-97, (2012).

[10] Reda, S. M. "Synthesis of ZnO and Fe2O3 nanoparticles by sol–gel method and their application in dye-sensitized solar cells." Materials Science in Semiconductor Processing., **13(5)**, 417-425, (2010).

[11] Kitaura, Hirokazu, Kenji Takahashi, Fuminori Mizuno, Akitoshi Hayashi, Kiyoharu Tadanaga, and Masahiro Tatsumisago. "Mechanochemical synthesis of α-Fe2O3 nanoparticles and their application to all-solid-state lithium batteries." Journal of Power Sources., **183(1)**, 418-421, (2008).

[12] Jiang, J. Z., Rong Lin, Weigang Lin, Kurt Nielsen, Steen Mørup, Kim Dam-Johansen, and R. Clasen. "Gas-sensitive properties and structure of nanostructured (-materials prepared by mechanical alloying." Journal of Physics D: Applied Physics., **30(10)**, 1459, (1997).

[13] Chi, Xiao, Changbai Liu, Li Liu, Shouchun Li, Haiying Li, Xiaobo Zhang, Xiaoqing Bo, and Hao Shan. "Enhanced formaldehyde-sensing properties of mixed Fe2O3–In2O3 nanotubes." Materials Science in Semiconductor Processing., **18**, 160-164, (2014).

[14] Walter, Dirk. "Characterization of synthetic hydrous hematite pigments." Thermochimica acta 445(2), 195-199, (2006).

[15] R.M. Cornell and U. Chwertmann, "The Iron Oxides", VCH Verlagsgesellschaft Weinheim Germany; VCH Publishers, New York., 463, (1996).

[16] Srivastava, Manish, Animesh K. Ojha, S. Chaubey, Jay Singh, Prashant K. Sharma, and Avinash C. Pandey. "Investigation on magnetic properties of α-Fe2O3 nanoparticles synthesized under surfactant-free condition by hydrothermal process." Journal of Alloys and Compounds., **500(2)**, 206-210, (2010).

[17] Shekhah, Osama, Wolfgang Ranke, Achim Schüle, Grigorios Kolios, and Robert Schlögl. "Styrene synthesis: high conversion over unpromoted iron oxide catalysts under practical working conditions." Angewandte Chemie International Edition., **42(46)**, 5760-5763, (2003).

[18] Jeong, Unyong, Xiaowei Teng, Yong Wang, Hong Yang, and Younan Xia. "Superparamagnetic colloids: controlled synthesis and niche applications." Advanced Materials., **19(1)**, 33-60, (2007).

[19] Pathan, Amanullakhan A., Kavita R. Desai, and Chandra P. Bhasin. "Improved Photocatalytic Properties of NiS Nanocomposites Prepared by Displacement Method for Removal of Rose Bengal Dye." Current Nanomaterials., **2(3)**, 169-176, (2017).

[20] Desai, K. R., A. A. Pathan, and C. P. Bhasin. "Synthesis, characterization of cadmium sulphide nanoparticles and its application as photocatalytic degradation of congored." Int J Nanomater Chem., **3**, 39, (2017).

[21] Mohammadikish, Maryam. "Hydrothermal synthesis, characterization and optical properties of ellipsoid shape α-Fe2O3 nanocrystals." Ceramics International., **40(1)**, 1351-1358, (2014).

[22] Khoshakhlagh, Ali, Ali Nazari, and Gholamreza Khalaj. "Effects of Fe2O3 nanoparticles on water permeability and strength assessments of high strength self-compacting concrete." Journal of Materials Science & Technology., **28(1)**, 73-82, (2012).

[23] Reda, S. M. "Synthesis of ZnO and Fe2O3 nanoparticles by sol–gel method and their application in dye-sensitized solar cells." Materials Science in Semiconductor Processing., **13(5)**, 417-425, (2010).

[24] He, Kai, Cheng-Yan Xu, Liang Zhen, and Wen-Zhu Shao. "Fractal growth of single-crystal α-Fe2O3: From dendritic micro-pines to hexagonal micro-snowflakes." Materials Letters., **62(4)**, 739-742, (2008).
[25] Chhabra, Vishal, Pushan Ayyub, Soma Chattopadhyay, and A. N. Maitra. "Preparation of acicular γ-Fe2O3 particles from a micro emulsion-mediated reaction." Materials Letters 26(1), 21-26, (1996).
[26] Tao, Bo, Qian Zhang, Zezhong Liu, and Baoyou Geng. "Cooperative effect of pH value and anions on single-crystalline hexagonal and circular α-Fe2O3 nanorings." Materials Chemistry and Physics., **136(2)**, 604-612, (2012).
[27] Wang, Li-Li, and Ji-Sen Jiang. "Preparation of α-Fe2O3 nanoparticles by high-energy ball milling." Physica B: Condensed Matter., **390(1)**, 23-27, (2007).
[28] Sun, Youyi, Binghua Yang, Ye Tian, Guizhen Guo, Wei Cai, Minghong He, and Yaqing Liu. "Facile synthesis of Ag–Fe2O3 core–shell composite nanoparticles by an in situ method." Micro & Nano Letters., **6(2)**, 82-85, (2011).
[29] Fu, Y. Y., R. M. Wang, J. Xu, J. Chen, Y. Yan, A. V. Narlikar, and H. Zhang. "Synthesis of large arrays of aligned α-Fe2O3 nanowires." Chemical Physics Letters., **379(3)**, 373-379, (2003).
[30] Pathan, Amanullakhan A., Kavita R. Desai, and C. P. Bhasin. "Synthesis of La2O3 Nanoparticles Using Glutaric Acid and Propylene Glycol for Future CMOS Applications." International journal of Nanomaterials and Chemistry., **3**, 21-25, (2017).
[31] Pathan, Amanullakhan A., Kavita R. Desai, Shailesh Vajapara, and C. P. Bhasin. "Conditional Optimization of Solution Combustion Synthesis for Pioneered La2O3 Nanostructures to Application as Future CMOS and NVMS Generations." Advances in Nanoparticles., **7(1)**, 28, (2018).
[31] Tejani, Jayadip, Rahul Shah, Hiral Vaghela, Trupti Kukadiya, and Amanullakhan A. Pathan. "Conditional Optimization of Displacement Synthesis for Pioneered ZnS Nanostructures." J Nanotech Adv Mater., **6(1)**, 1-7, (2018).
[32] Tejani, Jayadeep, Rahul Shah, Hiral Vaghela, Shailesh Vajapara, and Amanullakhan Pathan. "Controlled Synthesis and Characterization of Lanthanum Nanorods." Int. J. Thin. Film. Sci. Tec., **9(2)**, 119-125, (2020).
[33] Wang, Shurong, Liwei Wang, Taili Yang, Xianghong Liu, Jun Zhang, Baolin Zhu, Shoumin Zhang, Weiping Huang, and Shihua Wu. "Porous α-Fe2O3 hollow microspheres and their application for acetone sensor." Journal of Solid-State Chemistry., **183(12)**, 2869-2876, (2010).
[34] Zhang, Zhonghai, Md Faruk Hossain, and Takakazu Takahashi. "Fabrication of shape-controlled α-Fe2O3 nanostructures by sonoelectrochemical anodization for visible light photocatalytic application." Materials Letters., **64(3)**, 435-438, (2010).
[35] Maji, Swarup Kumar, Nillohit Mukherjee, Anup Mondal, and Bibhutosh Adhikary. "Synthesis, characterization and photocatalytic activity of α-Fe2O3 nanoparticles." Polyhedron., **33(1)**, 145-149, (2012).
[36] Hua, Jiao, and Jiao Gengsheng. "Hydrothermal synthesis and characterization of monodisperse α-Fe2O3 nanoparticles." Materials Letters., **63(30)**, 2725-2727, (2009).
[37] Jahagirdar, A. A., N. Dhananjaya, D. L. Monika, C. R. Kesavulu, H. Nagabhushana, S. C. Sharma, B. M. Nagabhushana, C. Shivakumara, J. L. Rao, and R. P. S. Chakradhar. "Structural, EPR, optical and magnetic properties of α-Fe2O3 nanoparticles." Spectrochimica Acta Part A: Molecular and Biomolecular Spectroscopy., **104**, 512-518, (2013).
[38] Wang, F., X. F. Qin, Y. F. Meng, Z. L. Guo, L. X. Yang, and Y. F. Ming. "Hydrothermal synthesis and characterization of α-Fe2O3 nanoparticles." Materials Science in Semiconductor Processing., **16(3)**, 802-806, (2013).
[39] Raja, K., M. Mary Jaculine, M. Jose, Sunil Verma, A. A. M. Prince, K. Ilangovan, K. Sethusankar, and S. Jerome Das. "Sol–gel synthesis and characterization of α-Fe2O3 nanoparticles." Superlattices and Microstructures., **86**, 306-312, (2015).
[40] English, Niall J., Mahfujur Rahman, Nitin Wadnerkar, and J. M. D. MacElroy. "Photo-active and dynamical properties of hematite (Fe2O3)–water interfaces: an experimental and theoretical study." Physical Chemistry Chemical Physics **16(28)**, 14445-14454, (2014).
[41] Lima, Sirlene B., Sarah Maria S. Borges, Maria do Carmo Rangel, and Sergio G. Marchetti. "Effect of iron content on the catalytic properties of activated carbon-supported magnetite derived from biomass." Journal of the Brazilian Chemical Society., **24(2)**, 344-354, (2013).
[42] Almeida, Trevor P., Mike Fay, Yanqiu Zhu, and Paul D. Brown. "Process map for the hydrothermal synthesis of α-Fe2O3 nanorods." The Journal of Physical Chemistry C., **113(43)**, 18689-18698, (2009).
[43] Zhang, Guo-Ying, Yan-Yan Xu, Dong-Zhao Gao, and Ya-Qiu Sun. "α-Fe2O3 nanoplates: PEG-600 assisted hydrothermal synthesis and formation mechanism." Journal of Alloys and Compounds., **509(3)**, 885-890, (2011).
[44] Zhang, Guo-Ying, Yan Feng, Yan-Yan Xu, Dong-Zhao Gao, and Ya-Qiu Sun. "Controlled synthesis of mesoporous α-Fe2O3 nanorods and visible light photocatalytic property." Materials Research Bulletin., **47(3)**, 625-630, (2012).
[45] Dhlamini, M. S., L. L. Noto, B. M. Mothudi, M. Chithambo, and L. E. Mathevula. "Structural and optical properties of sol-gel derived α-Fe2O3 nanoparticles." Journal of Luminescence., **192**, 879-887, (2017).
[46] Bandara, J., U. Klehm, and J. Kiwi. "Raschig rings-Fe2O3 composite photocatalyst activate in the degradation of 4-chlorophenol and Orange II under daylight irradiation." Applied Catalysis B: Environmental., **76(1)**, 73-81, (2007).
[47] Sherman, David M. "Electronic structures of iron (III) and manganese (IV) (hydr) oxide minerals: Thermodynamics of photochemical reductive dissolution in aquatic environments." Geochimica et Cosmochimica Acta., **69(13)**, 3249-3255, (2005).